

Dynamical theory of single-photon transport through a qubit chain coupled to a one-dimensional nanophotonic waveguide. Beyond the Markovian approximation

Ya. S. Greenberg,^{*} O. A. Chuikin, A. A. Shtygashev, and A. G. Moiseev
Novosibirsk State Technical University, Novosibirsk, Russia
 (Dated: July 28, 2023)

We study the dynamics of a single-photon pulse travelling through a linear qubit chain coupled to continuum modes in a one-dimensional (1D) photonic waveguide. We derive a time-dependent dynamical theory for qubits' amplitudes and for transmitted and reflected spectra. We show that the requirement for the photon-qubit coupling to exist only for positive frequencies can significantly change the dynamics of the system. First, it leads to the additional photon-mediated dipole-dipole interaction between qubits which results in the violation of the phase coherence between them. Second, the spectral lines of transmitted and reflected spectra crucially depend on the shape of incident pulse. We apply our theory to one-qubit and two-qubit systems. For these two cases we obtain the explicit expressions for the qubits' amplitudes and for the photon radiation spectra as time tends to infinity. For the incident Gaussian wave packet we calculate the line shapes of transmitted and reflected photons.

I. INTRODUCTION

Manipulating the propagation of photons in a one-dimensional waveguide coupled to an array of two-level atoms (qubits) may have important applications in quantum devices and quantum information technologies [1–4].

Quantum bits can be implemented with a variety of quantum systems, such as trapped ions [5], photons [6–8], and quantum dots [9, 10]. In particular, superconducting qubits [11, 12] have emerged as one of the leading candidate for scalable quantum processor architecture.

Transmission of a single photon through an array of two-level atoms embedded in a 1D open waveguide has been extensively studied both theoretically [13–15] and experimentally [16–18].

Most of theoretical calculations of the transmitted and reflected photon amplitudes in a 1D open waveguide with the atoms placed inside have been performed within a framework of the stationary theory in a configuration space [19–22] or by alternative methods such as those based on Lippmann-Schwinger scattering theory [23–25], the input-output formalism [14, 26, 27], the non-Hermitian Hamiltonian [28], and the matrix methods [29, 30].

Even though the stationary theory of the photon transport provides a useful guide to what one would expect in real experiment, it does not allow for a description of the dynamics of a qubit excitation and the evolution of the scattered photon amplitudes.

In practice, the qubits are excited by the photon pulses with finite duration and finite bandwidth. Therefore, to study the real time evolution of the photon transport and atomic excitation the time-dependent dynamical theory was developed [31–35]. The theory relies on two assumptions. The first one is the Wigner-Weisskopf approximation in which the rate of spontaneous emission

to the guided mode is much less than the qubit frequency, $\Gamma(\omega) \ll \Omega$. Therefore, the decay rate Γ is assumed frequency independent and is taken at the resonant frequency Ω , $\Gamma(\omega) = \Gamma(\Omega) \equiv \Gamma$. The second assumption is more tricky. It is assumed that the photon-mediated coupling $g(\omega)$ may be extended to negative frequencies which allows to move the lower bound of some frequency integrals to minus infinity. In this case, the transmitted and reflected photon amplitudes become proportional to the spectral density of incident pulse, $\gamma_0(\omega)$ [32]. It is believed that the continuation of $g(\omega)$ to negative frequencies is justified beyond rotating wave approximation (RWA) by accounting for counter rotating terms (see Supplement in [36]). The extension to negative frequencies are generally relies on the assumption that non-RWA contribution is negligible which is not always the case. Moreover, it is not justified from physical arguments: because the continuum starts at $\omega = 0$, the density of states is zero for $\omega < 0$. Therefore, $g(\omega) = 0$ for $\omega < 0$, that is the coupling does not exist at negative frequencies [37]. Thus, its continuation to negative frequencies makes no sense. From the other hand, we may consider this continuation as a pure mathematical trick which can be justified if the negative frequency integral provides a small correction. This is indeed the case if the distance between qubits d exceeds the qubit wavelength λ [38]. However, as is shown in this paper, if $d < \lambda$ the discrepancy can be significant.

Another consequence of "no continuation" of $g(\omega)$ to negative frequencies is more complicated dependence of photon radiation on the shape of incident pulse: the transmitted and reflected photon amplitudes are no longer proportional to $\gamma_0(\omega)$.

From the point of view of device applications, a control pulse generator should be placed as close as possible to the measured qubit circuitry, for example, in the same chip with superconducting qubit at millikelvin temperatures [39]. Here we show that such an arrangement leads to significant modifications of the photon radiation spectra.

^{*}Electronic address: yakovgreenberg@yahoo.com

The paper is organized as follows. In Section II we briefly describe our system consisting of N identical qubits in a one-dimensional infinite waveguide. The system is described by Jaynes-Cummings Hamiltonian in rotating wave approximation (RWA). The Hilbert space is restricted to the single-excitation subspace.

In Section III the general time-dependent equations for qubits' amplitudes, $\beta_n(t)$ and photon forward, $\gamma(\omega, t)$ and backward $\delta(\omega, t)$ radiation spectra are derived for the process of a single-photon pulse scattering by an array of N identical qubits. Next, we apply the Fourier transform method to obtain for Fourier amplitudes $\beta_n(\nu)$, $\gamma(\omega, \nu)$, $\delta(\omega, \nu)$ a set of linear algebraic equations which allow us to find the desired solutions for time-dependent amplitudes. The main result of this section is the additional quantity $G(kd)$ in the equations for qubits amplitudes. It is shown that $G(kd)$ is responsible for direct interqubit interaction which is not negligible if the distance between two qubits is less than the qubit wavelength.

The theoretical results obtained in Section III are applied for the calculations of photon forward and backward radiation spectra for scattering from one qubit (Section IV) and from two-qubit system (Section V). Summary of our work presented in conclusion (Section VI). Some additional calculations are placed in Appendixes.

II. THE MODEL

We consider a system consisting of N identical qubits in a one-dimensional infinite waveguide. In the continuum mode representation this system can be described by a Jaynes-Cummings Hamiltonian which accounts for the interaction between qubits and electromagnetic field [40, 41] (from now on we use the units $\hbar = 1$ throughout the paper, therefore, all energies are expressed in frequency units):

$$\begin{aligned}
 H = & \frac{1}{2} \sum_{n=1}^N \left(1 + \sigma_z^{(n)} \right) \Omega \\
 & + \int_0^\infty \omega a^\dagger(\omega) a(\omega) d\omega + \int_0^\infty \omega b^\dagger(\omega) b(\omega) d\omega \\
 & + \int_0^\infty a^\dagger(\omega) S_-(\omega) d\omega + \int_0^\infty a(\omega) S_+(\omega) d\omega \\
 & + \int_0^\infty b^\dagger(\omega) S_-^*(\omega) d\omega + \int_0^\infty b(\omega) S_+^*(\omega) d\omega,
 \end{aligned} \tag{1}$$

where $\sigma_z^{(n)}$ is a Pauli spin operator, Ω is a resonant frequency of n th qubit, ω is a photon frequency.

The photon creation and annihilation operators $a^\dagger(\omega)$, $a(\omega)$, and $b^\dagger(\omega)$, $b(\omega)$ describe forward and backward scattering waves, respectively. They are independent of each other and satisfy the usual continuous-mode com-

mutation relations [40]:

$$[a(\omega), a^\dagger(\omega')] = [b(\omega), b^\dagger(\omega')] = \delta(\omega - \omega'). \tag{2}$$

In (1) we introduced collective atomic spin operators:

$$\begin{aligned}
 S_-(\omega) &= \sum_{n=1}^N g(\omega) e^{-ikx_n} \sigma_-^{(n)}, \\
 S_+(\omega) &= \sum_{n=1}^N g(\omega) e^{ikx_n} \sigma_+^{(n)}.
 \end{aligned} \tag{3}$$

where $k = \omega/v_g$, v_g is the group velocity of electromagnetic waves, x_n is a spatial coordinate of the n th qubit. $\sigma_-^{(n)} = |g\rangle_{nn} \langle e|$ and $\sigma_+^{(n)} = |e\rangle_{nn} \langle g|$ are the lowering and raising atomic operators which lower or raise a state of the n th qubit. A spin operator $\sigma_z^{(n)} = |e\rangle_{nn} \langle e| - |g\rangle_{nn} \langle g|$. The quantity $g(\omega)$ in (1) is the coupling between qubit and the photon field in a waveguide [41]:

$$g(\omega) = \sqrt{\frac{\omega d^2}{4\pi\epsilon_0 \hbar v_g S}}, \tag{4}$$

where d is the off diagonal matrix element of a dipole operator, S is the effective transverse cross section of the modes in one-dimensional waveguide, v_g is the group velocity of electromagnetic waves. We assume that the coupling is the same for forward and backward waves.

Note that the dimension of the coupling constant $g(\omega)$ is not a frequency, ω but a square of frequency, $\sqrt{\omega}$, and, as it follows from (2), the dimension of creation and destruction operators is $1/\sqrt{\omega}$.

Below we consider a single-excitation subspace with either a single photon is in a waveguide and all qubits are in the ground state, or there are no photons in a waveguide with the only n th qubit in the chain being excited. Therefore, we truncate Hilbert space to the following states:

$$\begin{aligned}
 |G, 1_k\rangle &= |g_1, g_2, \dots, g_N\rangle \otimes |1_k\rangle; \\
 |n, 0_k\rangle &= |g_1, g_2, \dots, g_{n-1}, e_n, g_{n+1}, \dots, g_N\rangle \otimes |0_k\rangle;
 \end{aligned} \tag{5}$$

The Hamiltonian (1) preserves the number of excitations (number of excited qubits + number of photons). In our case the number of excitations is equal to one. Therefore, at any instant of time the system will remain within a single-excitation subspace.

The wave function of an arbitrary single-excitation state can then be written in the form:

$$\begin{aligned}
 \Psi(t) &= \sum_{n=1}^N \beta_n(t) e^{-i\Omega t} |n, 0\rangle \\
 &+ \int_0^\infty d\omega \gamma(\omega, t) e^{-i\omega t} a^\dagger(\omega) |G, 0\rangle \\
 &+ \int_0^\infty d\omega \delta(\omega, t) e^{-i\omega t} b^\dagger(\omega) |G, 0\rangle,
 \end{aligned} \tag{6}$$

where $\beta_n(t)$ is the amplitude of n th qubit, $\gamma(\omega, t)$ and $\delta(\omega, t)$ are single-photon amplitudes which are related to a spectral density of forward and backward radiation, respectively.

The function (6) at any time is normalized to unity:

$$\sum_{n=1}^N |\beta_n(t)|^2 + \int_0^\infty d\omega |\gamma(\omega, t)|^2 + \int_0^\infty d\omega |\delta(\omega, t)|^2 = 1. \quad (7)$$

The initial conditions are as follows: all qubits are unexcited at $t = 0$, $\beta_n(0) = 0$; reflected wave is absent, $\delta(\omega, 0) = 0$; transmitted wave $\gamma(\omega, 0) \equiv \gamma_0(\omega)$, where $\gamma_0(\omega)$ is the incident pulse which for a single scattering photon is assumed to be normalized to unity, $\int_0^\infty d\omega |\gamma_0(\omega)|^2 = 1$. It is worth mentioning here that we cannot consider the initial mixed state:

$$\Psi(0) = \sum_{n=1}^N \beta_n(0) e^{-i\Omega t} |n, 0\rangle + \int_0^\infty d\omega \gamma_0(\omega) e^{-i\omega t} a^\dagger(\omega) |G, 0\rangle, \quad (8)$$

with $\beta_n(0) \neq 0$, since it is not compatible with normalizing condition (7).

We note that as $t \rightarrow \infty$ the qubit amplitude $\beta_n(t) \rightarrow 0$, therefore the equation (7) reduces to:

$$\int_0^\infty d\omega |\gamma(\omega, t \rightarrow \infty)|^2 + \int_0^\infty d\omega |\delta(\omega, t \rightarrow \infty)|^2 = 1. \quad (9)$$

III. EQUATIONS FOR QUBITS' AND PHOTON AMPLITUDES

The Schroedinger equation $i \frac{d\Psi(t)}{dt} = H\Psi(t)$ yields the equations for the amplitudes:

$$\begin{aligned} \frac{d\beta_n}{dt} &= -i \int_0^\infty d\omega g(\omega) \gamma(\omega, t) e^{ikx_n} e^{-i(\omega-\Omega)t} \\ &\quad -i \int_0^\infty d\omega g(\omega) \delta(\omega, t) e^{-ikx_n} e^{-i(\omega-\Omega)t}, \end{aligned} \quad (10)$$

$$\frac{d\gamma(\omega, t)}{dt} = -ig(\omega) e^{i(\omega-\Omega)t} \sum_{n=1}^N \beta_n(t) e^{-ikx_n}, \quad (11)$$

$$\frac{d\delta(\omega, t)}{dt} = -ig(\omega) e^{i(\omega-\Omega)t} \sum_{n=1}^N \beta_n(t) e^{ikx_n}. \quad (12)$$

We assume the photon is incident from the left on the first qubit at $t = 0$, so that $\gamma(\omega, 0) \equiv \gamma_0(\omega)$ and $\gamma(\omega, t) = 0$ if $t \leq 0$, $\delta(\omega, t) = 0$ if $t \leq 0$. The qubit system is assumed

to be prepared at $t = 0$ so that all qubit amplitudes $\beta_n(t) = 0$ if $t \leq 0$.

Therefore, the formal solutions of equations (11) and (12) are as follows:

$$\gamma(\omega, t) = \gamma_0(\omega) - i \sum_{n=1}^N \int_0^t d\tau \beta_n(\tau) g(\omega) e^{i(\omega-\Omega)\tau} e^{-ikx_n}, \quad (13a)$$

$$\delta(\omega, t) = -i \sum_{n=1}^N \int_0^t d\tau \beta_n(\tau) g(\omega) e^{i(\omega-\Omega)\tau} e^{ikx_n}. \quad (13b)$$

Next, we multiply the equation (10) by $e^{i(\nu-\Omega)t}$ and integrate over t from zero to infinity. We obtain:

$$\begin{aligned} -i(\nu - \Omega)\beta_n(\nu) &= -i \int_0^\infty d\omega g(\omega) \gamma(\omega, \nu) e^{ikx_n} \\ &\quad -i \int_0^\infty d\omega g(\omega) \delta(\omega, \nu) e^{-ikx_n}, \end{aligned} \quad (14)$$

where:

$$\beta_n(\nu) = \int_0^\infty dt \beta_n(t) e^{i(\nu-\Omega)t}, \quad (15)$$

$$\gamma(\omega, \nu) = \int_0^\infty dt \gamma(\omega, t) e^{i(\nu-\omega)t}, \quad (16)$$

$$\delta(\omega, \nu) = \int_0^\infty dt \delta(\omega, t) e^{i(\nu-\omega)t}. \quad (17)$$

Because qubits' and photon amplitudes are zero at $t < 0$ we may safely set the lower bound of integrals in (15), (16), (17) to $-\infty$. Therefore, the time dependent qubits' and photon amplitudes can be expressed as the inverse Fourier transform of the quantities $\beta_n(\nu)$, $\gamma(\omega, \nu)$, $\delta(\omega, \nu)$:

$$\beta_n(t) = \int_{-\infty}^\infty \frac{d\nu}{2\pi} \beta_n(\nu) e^{-i(\nu-\Omega)t}, \quad (18)$$

$$\gamma(\omega, t) = \int_{-\infty}^\infty \frac{d\nu}{2\pi} \gamma(\omega, \nu) e^{-i(\nu-\omega)t}, \quad (19)$$

$$\delta(\omega, t) = \int_{-\infty}^\infty \frac{d\nu}{2\pi} \delta(\omega, \nu) e^{-i(\nu-\omega)t}. \quad (20)$$

Next, we multiply the equations (11) and (12) by $e^{i(\nu-\omega)t}$ and integrate over t from zero to infinity. We obtain:

$$-\gamma_0(\omega) - i(\nu - \omega)\gamma(\omega, \nu) = -ig(\omega) \sum_{n=1}^N \beta_n(\nu) e^{-ikx_n}, \quad (21)$$

$$-i(\nu - \omega)\delta(\omega, \nu) = -ig(\omega) \sum_{n=1}^N \beta_n(\nu) e^{ikx_n}. \quad (22)$$

Because both frequency variables ω and ν belong to the continuum we will solve the equations (21) and (22) using the general approach first developed in Heitler's papers and considered in detail in [42], and subsequently used for the study of light scattering by a dense ensemble of atoms [43–45]:

$$\gamma(\omega, \nu) = g(\omega) \sum_{n=1}^N \beta_n(\nu) e^{-ikx_n} \zeta(\nu - \omega) + i\gamma_0(\omega) \zeta(\nu - \omega), \quad (23)$$

$$\delta(\omega, \nu) = g(\omega) \sum_{n=1}^N \beta_n(\nu) e^{ikx_n} \zeta(\nu - \omega), \quad (24)$$

where we introduce a singular zeta function defined as:

$$\zeta(\nu - \omega) = -i\pi\delta(\nu - \omega) + P \frac{1}{\nu - \omega}. \quad (25)$$

In (25), $\delta(\nu - \omega)$ is a Dirac delta-function, and P is a Cauchy principal value.

Next we substitute $\gamma(\omega, \nu)$, $\delta(\omega, \nu)$ in (14) with their expressions (23) and (24). Thus, we obtain a set of linear equations which define the Fourier components of the qubits' amplitudes $\beta_n(\nu)$:

$$\begin{aligned} & \left(\nu - \Omega - 2 \int_0^\infty d\omega g^2(\omega) \zeta(\nu - \omega) \right) \beta_n(\nu) \\ & - 2 \sum_{n' \neq n}^N \beta_{n'}(\nu) \int_0^\infty d\omega g^2(\omega) \cos(k(x_n - x_{n'})) \zeta(\nu - \omega) \\ & = i \int_0^\infty d\omega g(\omega) \gamma_0(\omega) e^{ikx_n} \zeta(\nu - \omega). \end{aligned} \quad (26)$$

Using (25) in (26) we obtain:

$$\begin{aligned} & \left(\nu - \Omega - F(\nu) + i \frac{\Gamma(\nu)}{2} \right) \beta_n(\nu) \\ & + i \frac{\Gamma(\nu)}{2} \sum_{n' \neq n}^N \beta_{n'}(\nu) \left(e^{ik_\nu |x_n - x_{n'}|} + iG(k_\nu(x_n - x_{n'})) \right) \\ & = i \int_0^\infty d\omega g(\omega) \gamma_0(\omega) e^{ikx_n} \zeta(\nu - \omega), \end{aligned} \quad (27)$$

where (the derivation is given in Appendix A):

$$\begin{aligned} G(k_\nu d_{nn'}) &= -\frac{4}{\Gamma(\nu)} \int_0^\infty d\omega \frac{g^2(\omega) \cos k_\nu d_{nn'}}{\omega + \nu} \\ &= \frac{1}{\pi} \cos k_\nu d_{nn'} Ci(|k_\nu d_{nn'}|) \\ &+ \frac{1}{\pi} \sin k_\nu d_{nn'} \left(-\frac{\pi}{2} \text{sgn}(d_{nn'}) + Si(k_\nu d_{nn'}) \right), \end{aligned} \quad (28)$$

$d_{nn'} = x_n - x_{n'}$, $\Gamma(\nu) = 4\pi g^2(\nu)$, $F(\nu) = 2P \int_0^\infty \frac{g^2(\omega)}{\nu - \omega} d\omega$, $k_\nu = \nu/v_g$, $k = \omega/v_g$; $Ci(x)$ and $Si(x)$ are the cosine and sine integral functions:

$$Ci(x) = -\int_x^\infty dt \frac{\cos t}{t}, \quad Si(x) = \int_0^x dt \frac{\sin t}{t}. \quad (29)$$

Because $Ci(x)$ is defined for $x > 0$ and $Si(-x) = -Si(x)$, the quantity $G(x)$ is the even function, $G(-x) = G(x)$.

As the quantity $G(kd_{nn'})$ is a real function it modifies the interaction between qubits giving rise to the shift of their frequencies. We consider this property in more details in Section IV for two-qubit system.

From a set of linear equations (27) we can find N Fourier amplitudes $\beta_n(\nu)$. The next step is to find from (23) and (24) photon Fourier amplitudes $\gamma(\omega, \nu)$ and $\delta(\omega, \nu)$. Finally, from Fourier transform (18), (19) and (20) we find the qubits' and photon amplitudes in a time domain. The scattering amplitudes for $t \rightarrow \infty$ can be also found directly from (13a) and (13b) where $\beta_n(\omega)$ is the solution of (27):

$$\gamma(\omega, t \rightarrow \infty) = \gamma_0(\omega) - ig(\omega) \sum_{n=1}^N \beta_n(\omega) e^{-ikx_n}, \quad (30)$$

$$\delta(\omega, t \rightarrow \infty) = -ig(\omega) \sum_{n=1}^N \beta_n(\omega) e^{ikx_n}. \quad (31)$$

Below we will show the application of this method to the cases of one and two qubits in a waveguide for which the analytical solutions can be obtained in a closed form.

IV. SINGLE QUBIT

For a single two-level atom located at $x = 0$ the solution of equation (27) is given by:

$$\beta(\omega) = \frac{i \int_0^\infty d\omega' g(\omega') \gamma_0(\omega') \zeta(\omega - \omega')}{\left(\omega - \Omega - F(\omega) + i \frac{\Gamma(\omega)}{2} \right)}. \quad (32)$$

With the aid of (30) and (31) we calculate the transmitted and reflected photon amplitudes $\gamma(\omega, t \rightarrow \infty)$ and $\delta(\omega, t \rightarrow \infty)$:

$$\gamma(\omega, t \rightarrow \infty) = \gamma_0(\omega) \frac{\omega - \Omega - F(\omega) + i\frac{\Gamma(\omega)}{4}}{\omega - \Omega - F(\omega) + i\frac{\Gamma(\omega)}{2}} + \frac{g(\omega)P \int_0^\infty \frac{d\omega' g(\omega') \gamma_0(\omega')}{\omega - \omega'}}{\omega - \Omega - F(\omega) + i\frac{\Gamma(\omega)}{2}}, \quad (33)$$

$$\delta(\omega, t \rightarrow \infty) = \gamma_0(\omega) \frac{-i\frac{\Gamma(\omega)}{4}}{\omega - \Omega - F(\omega) + i\frac{\Gamma(\omega)}{2}} + \frac{g(\omega)P \int_0^\infty \frac{d\omega' g(\omega') \gamma_0(\omega')}{\omega - \omega'}}{\omega - \Omega - F(\omega) + i\frac{\Gamma(\omega)}{2}}. \quad (34)$$

As it is seen from (33) and (34) $\gamma(\omega, t \rightarrow \infty) - \delta(\omega, t \rightarrow \infty) = \gamma_0(\omega)$, the condition which is only valid for the scattering from a single qubit. The flux conservation is fulfilled not at a single frequency, but as integral quantity: (see normalizing condition (9)).

We note that the derivation of the transmitted and reflected amplitudes (33) and (34) is not restricted to Wigner-Weisskopf approximation $\Gamma(\Omega) \ll \Omega$. It is also valid for strong coupling where $\Gamma(\Omega) \leq \Omega$.

The evolution of qubit's amplitude $\beta(t)$ is obtained from (18) with $\beta(\omega)$ from (32):

$$\beta(t) = \int_{-\infty}^{\infty} \frac{d\omega}{2\pi} \frac{i \int_0^\infty d\omega' g(\omega') \gamma_0(\omega') \zeta(\omega - \omega')}{\omega - \Omega - F(\omega) + i\frac{\Gamma(\omega)}{2}} e^{-i(\omega - \Omega)t}. \quad (35)$$

In Wigner-Weisskopf approximation we can obtain a simple analytical expression for the evolution of qubit's amplitude (35) (see Appendix B):

$$\beta(t) = \int_0^\infty d\omega g(\omega) \gamma_0(\omega) \frac{e^{-\frac{\Gamma}{2}t} - e^{-i(\omega - \Omega)t}}{(\omega - \Omega + i\frac{\Gamma}{2})}. \quad (36)$$

The expressions (33), (34) look rather different from the transmitted and reflected amplitudes which were found in a framework of stationary scattering approach for a monochromatic signal scattered by a two-level atom in an 1D open waveguide [48, 49]:

$$\gamma(\omega) = \frac{\omega - \Omega}{\omega - \Omega + i\frac{\Gamma}{2}}, \quad (37)$$

$$\delta(\omega) = \frac{-i\frac{\Gamma}{2}}{(\omega - \Omega + i\frac{\Gamma}{2})}. \quad (38)$$

Below we show that in some cases the expressions (33) and (34) provide the stationary scattering results.

We assume that the incident wave packet is a narrow pulse which can be approximated by a delta function:

$$\gamma_0(\omega) = A\delta(\omega - \omega_S) = \frac{A}{2\pi} \int_{-\infty}^{+\infty} d\lambda e^{i\lambda(\omega - \omega_S)}. \quad (39)$$

Plugging (39) in (33) and (34) we obtain for principal value integral:

$$\begin{aligned} P \int_0^\infty d\omega' \frac{g(\omega') \gamma_0(\omega')}{\omega - \omega'} &\approx g(\omega) \frac{A}{2\pi} \int_{-\infty}^\infty d\lambda e^{-i\lambda\omega_S} P \int_{-\infty}^\infty d\omega' \frac{e^{i\lambda\omega'}}{\omega - \omega'} \\ &= -i\pi g(\omega) \frac{A}{2\pi} \int_{-\infty}^\infty d\lambda e^{-i\lambda\omega_S} e^{i\lambda\omega} = -i\pi g(\omega) A\delta(\omega - \omega_S) \\ &\equiv -i\pi g(\omega) \gamma_0(\omega). \end{aligned} \quad (40)$$

When deriving (40) we first assume that the coupling $g(\omega)$ is a slow function of ω , so that we take it out of the integral. Second, we put the lower bound in principal value integral to minus infinity which allows the application of Kramers-Kronig relation $P \int_{-\infty}^{+\infty} \frac{e^{i\lambda\omega'}}{\omega - \omega'} d\omega' = -i\pi e^{i\lambda\omega}$.

If we use the result (40) in (33) and (34) and assume that the atom is initially not excited, we obtain for transmitted and reflection amplitudes the expressions which are known from the stationary theories:

$$\gamma(\omega, t \rightarrow \infty) = \gamma_0(\omega) \frac{\omega - \Omega - F(\omega)}{\omega - \Omega - F(\omega) + i\frac{\Gamma(\omega)}{2}}, \quad (41)$$

$$\delta(\omega, t \rightarrow \infty) = \gamma_0(\omega) \frac{-i\frac{\Gamma(\omega)}{2}}{\omega - \Omega - F(\omega) + i\frac{\Gamma(\omega)}{2}}. \quad (42)$$

These expressions are similar to those obtained in the framework of time-dependent approach in [32], where $\gamma_0(\omega)$ was arbitrary pulse shape. However, here the expressions (41) and (42) are valid if the incident photon is a delta pulse (39). For this case, these expressions are exact asymptotic solutions for time dependent scattering of a single-photon pulse from a two-level atom [46].

For arbitrary shape of $\gamma_0(\omega)$ the exact expressions (33) and (34) must be used.

Below we present several plots for qubit's amplitude, forward and backward photon spectra calculated from expressions (36), (33), and (34) for incident travelling Gaussian pulse:

$$\gamma_0(\omega) = \left(\frac{2}{\pi \Delta^2} \right)^{1/4} \exp \left(i(\omega - \omega_S)t_0 - \frac{(\omega - \omega_S)^2}{\Delta^2} \right), \quad (43)$$

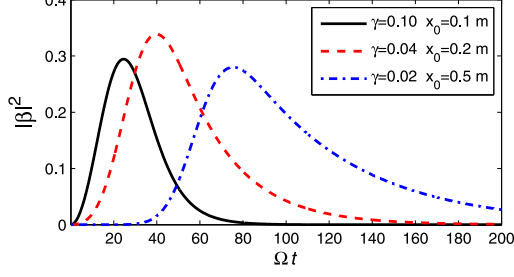


FIG. 1: Probability of the qubit excitation for different distances, x_0 of the maximum of incident Gaussian pulse from the qubit. $\Delta/\Omega = 0.1$, $\gamma = \Gamma/\Omega = 0.1$, solid black line; $\gamma = 0.04$, dashed red line; $\gamma = 0.02$, dashed-dotted blue line.

where Δ is the width of Gaussian pulse in the frequency domain, $t_0 = x_0/v_g$ is the time that it takes for the center of a Gaussian packet to travel from the point x_0 to the point $x = 0$ where the qubit is located.

We assume that at the initial time $t = 0$ qubit is in its ground state and the maximum of the envelope of a Gaussian pulse is located at the distance x_0 from the qubit. The plots of qubit's excitation probability $|\beta|^2$ for three values of initial distance x_0 between Gaussian pulse and qubit are shown in Fig. 1 for $\Delta/\Omega = 0.1$ and three values for decay rates $\gamma = \Gamma/\Omega = 0.02, 0.04, 0.1$. It is clearly seen that the qubit decay rates depend on γ : the lower γ the longer the qubit decays. Our calculations (not shown here) show that the maximum excitation, $|\beta_{max}|^2 \approx 0.38$, is obtained if $\Delta = \Gamma$ no matter how far the pulse is initially from the qubit. Similar result ($|\beta_{max}|^2 = 0.4$) was obtained in [31] where the position of the peak of the pulse at $t = 0$ was at the distance $10v_g/\Gamma$ from the qubit.

We rewrite (33) and (34) in Wigner-Weisskopf approximation, $\Gamma(\omega) = \Gamma(\Omega) \equiv \Gamma$, $g(\omega) = g(\Omega) = (\Gamma/4\pi)^{1/2}$. The frequency shift $F(\omega) = F(\Omega)$ is incorporated implicitly in Ω .

$$\gamma_{WW}(\omega) = \gamma_0(\omega) \frac{\omega - \Omega + i\frac{\Gamma}{4}}{\omega - \Omega + i\frac{\Gamma}{2}} + \frac{\frac{\Gamma}{4\pi} P \int_0^\infty \frac{d\omega' \gamma_0(\omega')}{\omega - \omega'}}{\omega - \Omega + i\frac{\Gamma}{2}}, \quad (44)$$

$$\delta_{WW}(\omega) = \gamma_0(\omega) \frac{-i\frac{\Gamma}{4}}{\omega - \Omega + i\frac{\Gamma}{2}} + \frac{\frac{\Gamma}{4\pi} P \int_0^\infty \frac{d\omega' \gamma_0(\omega')}{\omega - \omega'}}{\omega - \Omega + i\frac{\Gamma}{2}}. \quad (45)$$

We compare these expressions with those obtained in [32] for arbitrary pulse shape and with the extension of the coupling to negative frequencies:

$$\gamma(\omega) = \gamma_0(\omega) \frac{\omega - \Omega}{\omega - \Omega + i\frac{\Gamma}{2}}, \quad (46)$$

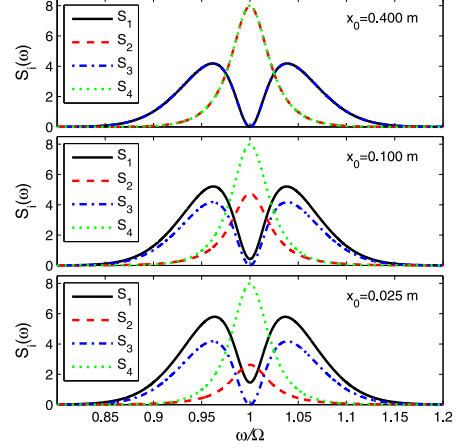


FIG. 2: Photon radiation spectra for different distances of the Gaussian peak from the qubit. $S_1(\omega) = |\gamma_{WW}(\omega)|^2 \Omega$, solid (black) line; $S_2(\omega) = |\delta_{WW}(\omega)|^2 \Omega$, dashed (red) line; $S_3(\omega) = |\gamma(\omega)|^2 \Omega$, dashed-dotted (blue) line; $S_4(\omega) = |\delta(\omega)|^2 \Omega$, dotted (green) line. The parameters of the qubit system and initial pulse are as follows: $\omega_S/\Omega = 1$, $\Gamma/\Omega = 0.05$, $\Delta/\Omega = 0.1$.

$$\delta(\omega) = \gamma_0(\omega) \frac{-i\frac{\Gamma}{2}}{\omega - \Omega + i\frac{\Gamma}{2}}. \quad (47)$$

First, we study how the photon spectra depend on the distance x_0 of a Gaussian peak from qubit. This behavior is shown in Fig.2. For relative large distance, $x_0 = 0.4$ m, the exact equations (44) and (45) provide practically the same result as the approximate equations (46) and (47). As the Gaussian peak becomes closer to the qubit the spectral lines more and more deviates from large distance results. Finally, we obtain the photon spectra for $x_0 = 0$ as shown in Fig.3.

Below in Fig.3, Fig.4, Fig.5 and Fig.6 we plot the forward, $S_1(\omega) = |\gamma_{WW}(\omega)|^2 \Omega$ and backward, $S_2(\omega) = |\delta_{WW}(\omega)|^2 \Omega$ radiation spectra calculated from exact expressions (44) and (45), and systematically compare them with those calculated from (46), $S_3(\omega) = |\gamma(\omega)|^2 \Omega$, and (47), $S_4(\omega) = |\delta(\omega)|^2 \Omega$. If it is not specified explicitly, all spectra are calculated for $x_0 = 0$.

The equations (46) and (47) provide the flux conservation at every frequency: $|\gamma(\omega)|^2 + |\delta(\omega)|^2 = |\gamma_0(\omega)|^2$. However, this simple condition is not valid for exact equations (44) and (45) where the normalization condition has the form of integral quantity (9). For every plot in Fig.3-Fig.6 we calculated the normalizing quantity $I = \int d\omega |\gamma_{WW}(\omega)|^2 + \int d\omega |\delta_{WW}(\omega)|^2$ where the integration was performed within the frequency span of the plots. In every case, I differs from unity less than a percent.

The major difference between the plots of equations (44), (45) and those of equations (46), (47) is that the transmittance $|\gamma_{WW}(\omega)|^2$ never equals zero at the reso-

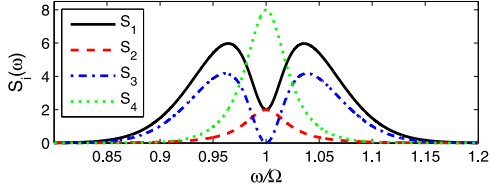


FIG. 3: Photon radiation spectra for scattering of Gaussian pulse (43) by a single qubit, $S_1(\omega) = |\gamma_{WW}(\omega)|^2\Omega$, solid (black) line; $S_2(\omega) = |\delta_{WW}(\omega)|^2\Omega$, dashed (red) line; $S_3(\omega) = |\gamma(\omega)|^2\Omega$, dashed-dotted (blue) line; $S_4(\omega) = |\delta(\omega)|^2\Omega$, dotted (green) line. The parameters of the qubit system and initial pulse are as follows: $\omega_S/\Omega = 1$, $\Gamma/\Omega = 0.05$, $\Delta/\Omega = 0.1$.

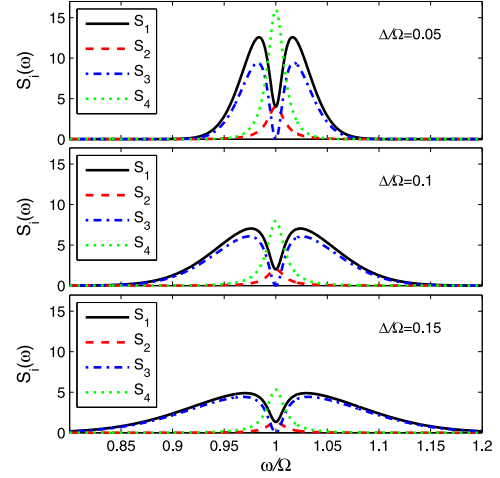


FIG. 5: Photon radiation spectra for scattering of Gaussian pulse (43) by a single qubit, $S_1(\omega) = |\gamma_{WW}(\omega)|^2\Omega$, solid (black) line; $S_2(\omega) = |\delta_{WW}(\omega)|^2\Omega$, dashed (red) line; $S_3(\omega) = |\gamma(\omega)|^2\Omega$, dashed-dotted (blue) line; $S_4(\omega) = |\delta(\omega)|^2\Omega$, dotted (green) line. The parameters of the qubit system and initial pulse are as follows: $\omega_S/\Omega = 1$, $\Gamma/\Omega = 0.02$.

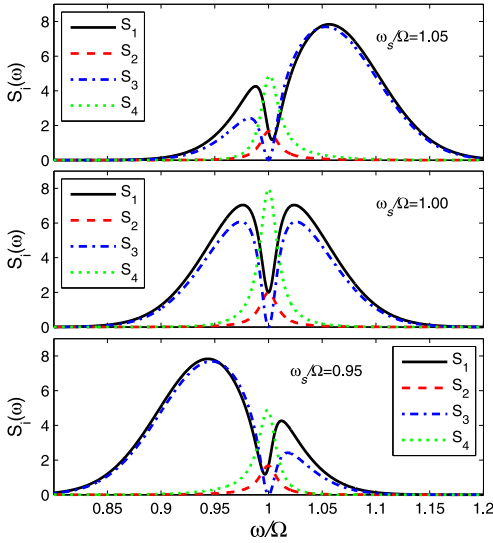


FIG. 4: Photon radiation spectra for scattering of Gaussian pulse (43) by a single qubit, $S_1(\omega) = |\gamma_{WW}(\omega)|^2\Omega$, solid (black) line; $S_2(\omega) = |\delta_{WW}(\omega)|^2\Omega$, dashed (red) line; $S_3(\omega) = |\gamma(\omega)|^2\Omega$, dashed-dotted (blue) line; $S_4(\omega) = |\delta(\omega)|^2\Omega$, dotted (green) line. The parameters of the qubit system and initial pulse are as follows: $\Delta/\Omega = 0.1$, $\Gamma/\Omega = 0.02$.

nance frequency, $\omega = \Omega$ and the reflectance $|\delta_{WW}(\omega)|^2$ never reaches its maximum value $|\gamma_0(\Omega)|^2$. These are the principal part integrals in (44), (45) which are responsible for these properties. From the other hand, the shape of the lines are similar. The transmittance $|\gamma_{WW}(\omega)|^2$ is up shifted relative to $|\gamma(\omega)|^2$, while the reflectance $|\delta_{WW}(\omega)|^2$ is down shifted relative to $|\gamma(\omega)|^2$.

V. TWO-QUBIT SYSTEM

In this section, we study how a single-photon pulse is scattered by a two-atom system coupled to a 1D wave-

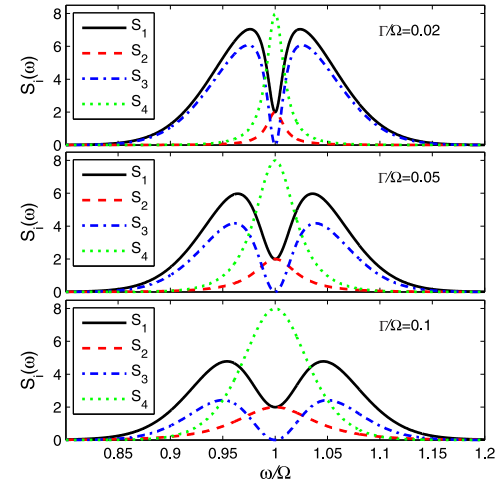


FIG. 6: Photon radiation spectra for scattering of Gaussian pulse (43) by a single qubit, $S_1(\omega) = |\gamma_{WW}(\omega)|^2\Omega$, solid (black) line; $S_2(\omega) = |\delta_{WW}(\omega)|^2\Omega$, dashed (red) line; $S_3(\omega) = |\gamma(\omega)|^2\Omega$, dashed-dotted (blue) line; $S_4(\omega) = |\delta(\omega)|^2\Omega$, dotted (green) line. The parameters of the qubit system and initial pulse are as follows: $\omega_S/\Omega = 1$, $\Delta/\Omega = 0.1$.

uide. We consider two atoms located at the coordinates $x_1 = 0$ and $x_2 = d$. From equations (27) we obtain two coupled equations for Fourier components of qubits' am-

plitudes $\beta_1(\nu)$ and $\beta_2(\nu)$:

$$\left(\Delta(\nu) + i\frac{\Gamma(\nu)}{2}\right)\beta_1(\nu) + i\frac{\Gamma(\nu)}{2}\beta_2(\nu)(e^{ik_\nu d} + iG(k_\nu d)) = C_1(\nu), \quad (48a)$$

$$\left(\Delta(\nu) + i\frac{\Gamma(\nu)}{2}\right)\beta_2(\nu) + i\frac{\Gamma(\nu)}{2}\beta_1(\nu)(e^{ik_\nu d} + iG(k_\nu d)) = C_2(\nu), \quad (48b)$$

where $\Delta(\nu) = \nu - \Omega - F(\nu)$, and:

$$C_1(\nu) = \pi g(\nu)\gamma_0(\nu) + iP \int_0^\infty d\omega \frac{g(\omega)\gamma_0(\omega)}{\nu - \omega}, \quad (49a)$$

$$C_2(\nu) = \pi g(\nu)\gamma_0(\nu)e^{ik_\nu d} + iP \int_0^\infty d\omega \frac{g(\omega)\gamma_0(\omega)e^{ik_\omega d}}{\nu - \omega}. \quad (49b)$$

From (48a) we find the explicit expressions for qubits' amplitudes:

$$\beta_1(\nu) = \frac{\left(\Delta(\nu) + i\frac{\Gamma(\nu)}{2}\right)C_1(\nu)}{\left(\Delta(\nu) + i\frac{\Gamma(\nu)}{2}\right)^2 + \frac{\Gamma^2(\nu)}{4}(e^{ik_\nu d} + iG(k_\nu d))^2} - \frac{i\frac{\Gamma(\nu)}{2}(e^{ik_\nu d} + iG(k_\nu d))C_2(\nu)}{\left(\Delta(\nu) + i\frac{\Gamma(\nu)}{2}\right)^2 + \frac{\Gamma^2(\nu)}{4}(e^{ik_\nu d} + iG(k_\nu d))^2}, \quad (50a)$$

$$\beta_2(\nu) = \frac{\left(\Delta(\nu) + i\frac{\Gamma(\nu)}{2}\right)C_2(\nu)}{\left(\Delta(\nu) + i\frac{\Gamma(\nu)}{2}\right)^2 + \frac{\Gamma^2(\nu)}{4}(e^{ik_\nu d} + iG(k_\nu d))^2} - \frac{i\frac{\Gamma(\nu)}{2}(e^{ik_\nu d} + iG(k_\nu d))C_1(\nu)}{\left(\Delta(\nu) + i\frac{\Gamma(\nu)}{2}\right)^2 + \frac{\Gamma^2(\nu)}{4}(e^{ik_\nu d} + iG(k_\nu d))^2}, \quad (50b)$$

where:

$$G(k_\nu d) = \frac{1}{\pi} \cos k_\nu d C i(k_\nu d) + \frac{1}{\pi} \sin k_\nu d \left(-\frac{\pi}{2} + Si(k_\nu d)\right). \quad (51)$$

From (30), (31) we obtain the scattering amplitudes for $t \rightarrow \infty$:

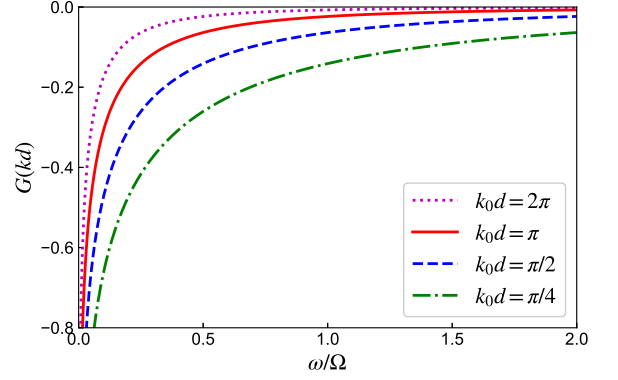


FIG. 7: The frequency dependence of $G(kd)$ for several interqubit distances $d = \lambda, \lambda/2, \lambda/4, \lambda/8$.

$$\begin{aligned} \gamma(\omega, t \rightarrow \infty) &= \gamma_0(\omega) \\ -ig(\omega) &\frac{\left(\Delta(\omega) + \frac{\Gamma}{2}e^{-ikd}G(kd)\right)C_1(\omega)}{\left(\Delta(\omega) + i\frac{\Gamma}{2}\right)^2 + \frac{\Gamma^2}{4}(e^{ikd} + iG(kd))^2} \\ -ig(\omega) &\frac{\left(\Delta(\omega)e^{-ikd} + \Gamma \sin kd + \frac{\Gamma}{2}G(kd)\right)C_2(\omega)}{\left(\Delta(\omega) + i\frac{\Gamma}{2}\right)^2 + \frac{\Gamma^2}{4}(e^{ikd} + iG(kd))^2}, \end{aligned} \quad (52)$$

$$\begin{aligned} i\delta(\omega, t \rightarrow \infty)e^{-ikd}/g(\omega) &= \frac{\left(\Delta(\omega) + \frac{\Gamma}{2}e^{-ikd}G(kd)\right)C_2(\omega)}{\left(\Delta(\omega) + i\frac{\Gamma}{2}\right)^2 + \frac{\Gamma^2}{4}(e^{ikd} + iG(kd))^2} \\ + \frac{\left(\Delta(\omega)e^{-ikd} + \Gamma \sin kd + \frac{\Gamma}{2}G(kd)\right)C_1(\omega)}{\left(\Delta(\omega) + i\frac{\Gamma}{2}\right)^2 + \frac{\Gamma^2}{4}(e^{ikd} + iG(kd))^2}, \end{aligned} \quad (53)$$

where $k = \omega/v_g$, $\Gamma \equiv \Gamma(\omega)$, and $C_1(\omega)$, $C_2(\omega)$ are given in (49a), (49b).

We also note here that the derivation of the transmitted and reflected amplitudes (52) and (53) is not restricted to Wigner-Weisskopf approximation $\Gamma(\Omega) \ll \Omega$. It is also valid for strong coupling where $\Gamma(\Omega) \leq \Omega$.

A. The properties of $G(kd)$

From the denominator in (50a),(50b) we find the equations for the resonances (poles) which lie in the lower part of the complex ω plane:

$$\begin{aligned} \Delta_-(\omega) &= -\frac{\Gamma(\omega)}{2}(\sin kd + G(kd)) - i\frac{\Gamma(\omega)}{2}(1 - \cos kd), \\ \Delta_+(\omega) &= \frac{\Gamma(\omega)}{2}(\sin kd + G(kd)) - i\frac{\Gamma(\omega)}{2}(1 + \cos kd), \end{aligned} \quad (54)$$

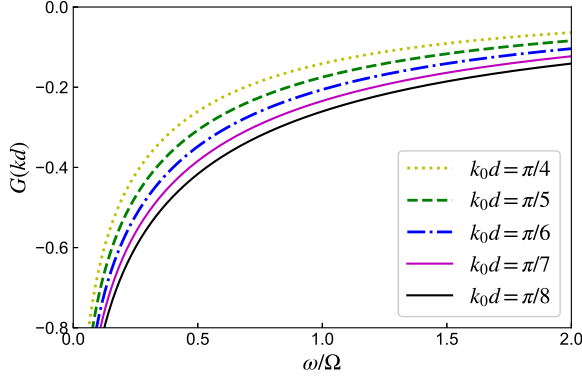


FIG. 8: The frequency dependence of $G(kd)$ in the range $-0.8 < G(kd) < 0$ for several interqubit distances $d = \lambda/8, \lambda/10, \lambda/12, \lambda/14, \lambda/16$.

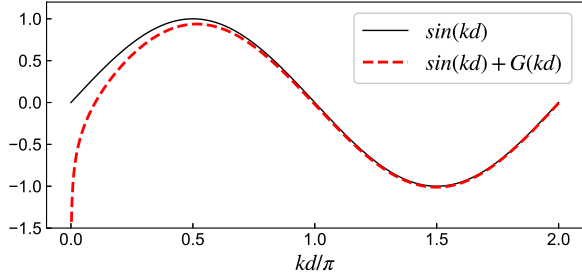


FIG. 9: The difference between $\sin(kd)$ and $\sin(kd) + G(kd)$ vs. kd for frequency $\omega = \Omega$.

where $k = \omega/v_g$. The numerical calculations show that in a vast range of relevant parameters the value $G(kd)$ is rather small (see Fig.7). A noticeable difference between $\sin(kd)$ and $\sin(kd) + G(kd)$ is only observed for $kd < \pi/2$. (see Fig.9). Therefore, for small $k_0d = \Omega d/v_g$ the main contribution to the frequency shift originates from $G(kd)$.

The number of poles depends on the interqubit distance d . Assuming Wigner-Weisskopf approximation, $\Gamma(\Omega)/\Omega \ll 1$ we may safely replace in the right hand side of equations (54) the running frequency ω with the qubit frequency Ω . Thus, in the plane of complex ω we obtain two poles:

$$\omega_{\pm} = \Omega + \Delta\Omega_{\pm} - i\Gamma_{\pm}, \quad (55)$$

where $\Delta\Omega_{\pm}$ is the frequency shift:

$$\Delta\Omega_{\pm} = F(\Omega) \pm \frac{\Gamma(\Omega)}{2} (\sin k_0d + G(k_0d)), \quad (56)$$

and Γ_{\pm} is the rate of spontaneous emission:

$$\Gamma_{\pm} = \frac{\Gamma(\Omega)}{2} (1 \pm \cos(k_0d)), \quad (57)$$

where $k_0 = \Omega/v_g$.

This two-pole approximation is also called Markovian approximation. It means that we may neglect the retardation effects: two qubits feel the incident photon instantaneously. As was shown in [22] the Markovian approximation is still valid for $k_0d < 5\pi$.

The non-Markovian regime is described by (54) where ω is the running frequency of incident photon. These equations imply that the resonance energies and their widths depend on the frequency of incident photon, which comes in (54) via the wave vector $k = \omega/v_g$. This is a general feature of non-Markovian behavior when the photon-mediated interaction between qubits is not instantaneous and the retardation effects have to be included. In our method the retardation effects are automatically included since the quantity kd explicitly enters the expressions for the transmission and reflection amplitudes. It is also common to disregard the frequency dependence of spontaneous emission rate Γ keeping it constant. In this case, non-Markovian behavior manifests via the wave vector $k = \omega/v_g$ [22].

From (56) we see that $G(k_0d)$ is responsible for the frequency shift, therefore, it modifies the interqubit interaction. As is seen from (56) we cannot switch off the interaction between two qubits taking $k_0d = n\pi$, where n is integer. However, for the values k_0d for which $\sin(k_0d) = 0$ this shift is rather small, $\Delta\Omega_{\pm}/\Gamma(\Omega) \ll 1$. On the other hand, for $k_0d \ll 1$, $G(k_0d)$ scales as $1/k_0d$. Therefore, in this case, the contribution from $G(k_0d)$ becomes essential. For example, for $k_0d = 0.01$, $G(0.01) = -1.28$. In this case, $\Delta\Omega_{\pm}/\Gamma(\Omega) = \pm 0.64$. This effect is the evidence of direct dipole-dipole interaction for which low frequency photons are responsible [50].

B. Photon amplitudes

As in the case of a single atom, we can show here that in the frame of Wigner-Weisskopf approximation and for narrow incident pulse the equations (52) and (53) provide the transmitted and reflected amplitudes which are known from the stationary scattering theories.

The calculation of $C_1(\omega)$ (49a) and $C_2(\omega)$ (49b) for a delta pulse (39) is similar to that of a single atom (40):

$$\begin{aligned} C_1(\omega) &= 2\pi g(\omega)\gamma_0(\omega), \\ C_2(\omega) &= 2\pi g(\omega)\gamma_0(\omega)e^{ik_{\omega}d}. \end{aligned} \quad (58)$$

Then, assuming the qubits are initially in the ground state and using the equations (30) and (31) we obtain the transmission and reflection spectra for two-qubit system in the Wigner-Weisskopf approximation:

$$\begin{aligned} \gamma(\omega, t \rightarrow \infty) &= \gamma_0(\omega) \frac{\Delta_0^2 - \frac{\Gamma^2}{4} G^2(kd) + i\frac{\Gamma^2}{2} (1 - \cos kd) G(kd)}{(\Delta_0 + i\frac{\Gamma}{2})^2 + \frac{\Gamma^2}{4} (e^{ikd} + iG(kd))^2}, \end{aligned} \quad (59)$$

$$\begin{aligned} \delta(\omega, t \rightarrow \infty) &= -i \frac{\Gamma}{2} \gamma_0(\omega) e^{ikd} \\ &\times \frac{2\Delta_0 \cos kd + \Gamma \sin kd + \Gamma G(kd)}{(\Delta_0 + i \frac{\Gamma}{2})^2 + \frac{\Gamma^2}{4} (e^{ikd} + iG(kd))^2}, \end{aligned} \quad (60)$$

where $\Delta_0 = \omega - \Omega$, $\gamma_0(\omega)$ is the incident delta pulse (39) and $\Gamma \equiv \Gamma(\Omega)$.

Further simplification can be obtained if the distance between qubits is sufficiently large, $kd \gg \pi$. For this case, within a width of the resonance line the quantity $|G(kd)| \ll 1$ (see Fig.7). Hence, we may disregard $G(kd)$ in the expressions (59) and (60):

$$\gamma(\omega, t \rightarrow \infty) = \gamma_0(\omega) \frac{(\omega - \Omega)^2}{(\omega - \Omega + i \frac{\Gamma}{2})^2 + \frac{\Gamma^2}{4} e^{2ik_\omega d}}, \quad (61)$$

$$\begin{aligned} \delta(\omega, t \rightarrow \infty) &= -i \frac{\Gamma}{2} \gamma_0(\omega) e^{ik_\omega d} \\ &\times \frac{2(\omega - \Omega) \cos(k_\omega d) + \Gamma \sin(k_\omega d)}{(\omega - \Omega + i \frac{\Gamma}{2})^2 + \frac{\Gamma^2}{4} e^{2ik_\omega d}}. \end{aligned} \quad (62)$$

The Markovian approximation is obtained by replacement k_ω with k_Ω in (59), (60), and (61), (62).

The expressions (61), (62) coincide with those obtained in [32] for arbitrary shape $\gamma_0(\omega)$ of the incident pulse and with the extension of the coupling to negative frequencies.

Here we calculate from equations (52) and (53) photon forward, $\gamma(\omega, t \rightarrow \infty)$ and backward, $\delta(\omega, t \rightarrow \infty)$ scattering amplitudes. For simplicity in these equations we assume the rate of spontaneous emission is constant, $\Gamma(\omega) = \Gamma(\Omega) \equiv \Gamma$. However, the non-Markovian non-linear dynamics still exists, since the expressions (52) and (53) depends on photon frequency via $k = \omega/v_g$. Therefore, the expressions (52) and (53) transform as follows:

$$\begin{aligned} \gamma_{WW}(\omega, t \rightarrow \infty) &= \gamma_0(\omega) \\ &- \frac{\Gamma}{4} \frac{(\omega - \Omega + \frac{\Gamma}{2} e^{-ikd} G(kd)) \left(i\gamma_0(\omega) + \frac{1}{\pi} P \int_0^\infty d\omega' \frac{\gamma_0(\omega')}{\omega' - \omega} \right)}{(\omega - \Omega + i \frac{\Gamma}{2})^2 + \frac{\Gamma^2}{4} (e^{ikd} + iG(kd))^2} \\ &- \frac{\Gamma}{4} \frac{((\omega - \Omega) e^{-ikd} + \Gamma \sin kd + \frac{\Gamma}{2} G(kd)) \left(i\gamma_0(\omega) e^{ikd} + \frac{1}{\pi} P \int_0^\infty d\omega' \frac{\gamma_0(\omega') e^{ik'd}}{\omega' - \omega} \right)}{(\omega - \Omega + i \frac{\Gamma}{2})^2 + \frac{\Gamma^2}{4} (e^{ikd} + iG(kd))^2}, \end{aligned} \quad (63)$$

$$\begin{aligned} \delta_{WW}(\omega, t \rightarrow \infty) &= -e^{ikd} \frac{\Gamma}{4} \frac{(\omega - \Omega + \frac{\Gamma}{2} e^{-ikd} G(kd)) \left(i\gamma_0(\omega) e^{ikd} + \frac{1}{\pi} P \int_0^\infty d\omega' \frac{\gamma_0(\omega') e^{ik'd}}{\omega' - \omega} \right)}{(\omega - \Omega + i \frac{\Gamma}{2})^2 + \frac{\Gamma^2}{4} (e^{ikd} + iG(kd))^2} \\ &- e^{ikd} \frac{\Gamma}{4} \frac{((\omega - \Omega) e^{-ikd} + \Gamma \sin kd + \frac{\Gamma}{2} G(kd)) \left(i\gamma_0(\omega) + \frac{1}{\pi} P \int_0^\infty d\omega' \frac{\gamma_0(\omega')}{\omega' - \omega} \right)}{(\omega - \Omega + i \frac{\Gamma}{2})^2 + \frac{\Gamma^2}{4} (e^{ikd} + iG(kd))^2}. \end{aligned} \quad (64)$$

Below we plot the forward and backward radiation spectra calculated from expressions (63) and (64), and compare them with those calculated from the expressions (61), (62) obtained in [32].

Similar to the one-qubit case, here the photon spectra also depend on the distance x_0 of a Gaussian peak from qubit. This behavior is shown in Fig.10 for $k_0 d = \pi/2$. For relative large distance, $x_0 = 0.5$ m, the exact equations (63) and (64) provide practically the same results as those of approximate equations (61) and (62). As the

Gaussian peak becomes closer to the first qubit the spectral lines more and more deviates from large distance results. Finally, we obtain the photon spectra for $x_0 = 0$ as shown in the middle panel in Fig.11.

All photon spectra which are shown in Fig.11-Fig.15 are calculated for the limiting case $x_0 = 0$.

Fig. 11 shows transmitted and reflected spectra for different inter-qubit distances $k_0 d = \pi, \pi/2, \pi/4$, which correspond to wavelengths $\lambda/2, \lambda/4$, and $\lambda/8$, respectively. The black solid line depicts transmitted spec-

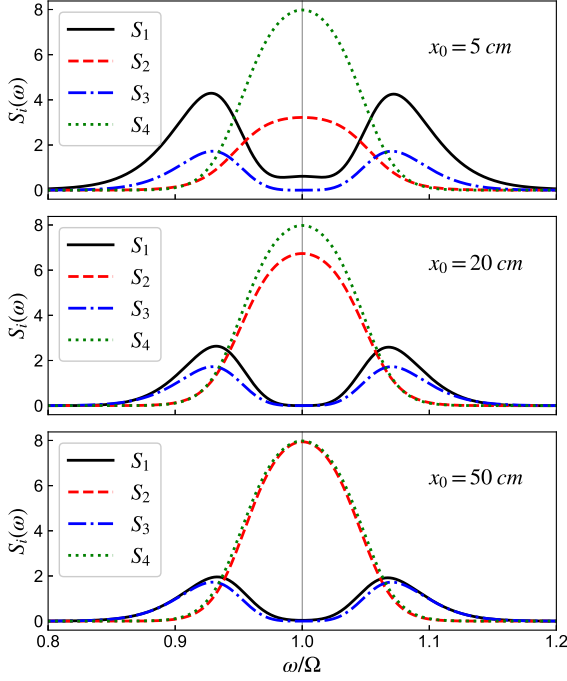


FIG. 10: Photon radiation spectra for different distances of the Gaussian peak from the first qubit for $k_0d = \pi/2$. $S_1(\omega) = |\gamma_{WW}(\omega)|^2\Omega$, solid (black) line; $S_2(\omega) = |\delta_{WW}(\omega)|^2\Omega$, dashed (red) line; $S_3(\omega) = |\gamma(\omega)|^2\Omega$, dashed-dotted (blue) line; $S_4(\omega) = |\delta(\omega)|^2\Omega$, dotted (green) line. The parameters of the qubit system and initial pulse are as follows: $\omega_S/\Omega = 1$, $\Gamma/\Omega = 0.1$, $\Delta/\Omega = 0.1$.

trum calculated from (63), $S_1 = |\gamma_{WW}(\omega, t \rightarrow \infty)|^2\Omega$, and the red dashed line shows reflected spectrum (64), $S_2 = |\delta_{WW}(\omega, t \rightarrow \infty)|^2\Omega$. The blue dash-dotted line and green dotted line are the transmitted and reflected spectra calculated from (61) and (62), respectively: $S_3 = |\gamma(\omega, t \rightarrow \infty)|^2\Omega$, $S_4 = |\delta(\omega, t \rightarrow \infty)|^2\Omega$.

As one can see from Fig. 11, the transmitted spectrum S_3 always has zero dip at center frequency $\omega/\Omega = 1$, which corresponds to full reflection of incident photon pulse from two-qubit system at resonant frequency. This is true for any inter-qubit length k_0d . The transmitted spectra S_1 and S_3 have always two distinct peaks, although they can be of different sizes, like S_1 for $k_0d = \pi/4$ at the last plot. The reflection spectra S_2 and S_4 , on the other hand, are represented by a single peak with maximum at resonant frequency. However, the exact transmitted spectrum S_1 never reaches zero at resonance frequency. We also note the appearance of a faint peak at the center frequency of the transmitted spectrum S_1 .

It is interesting to see how this central peak depends on other parameters of qubit system and initial photon pulse. In Fig. 12 we lock to the case of $k_0d = \pi/2$ and plot the same transmitted and reflected spectra for different coupling strength Γ/Ω . When the coupling is relatively small, $\Gamma/\Omega = 0.02$, central peak is quite sharp and clearly can be seen, despite its small size compared to

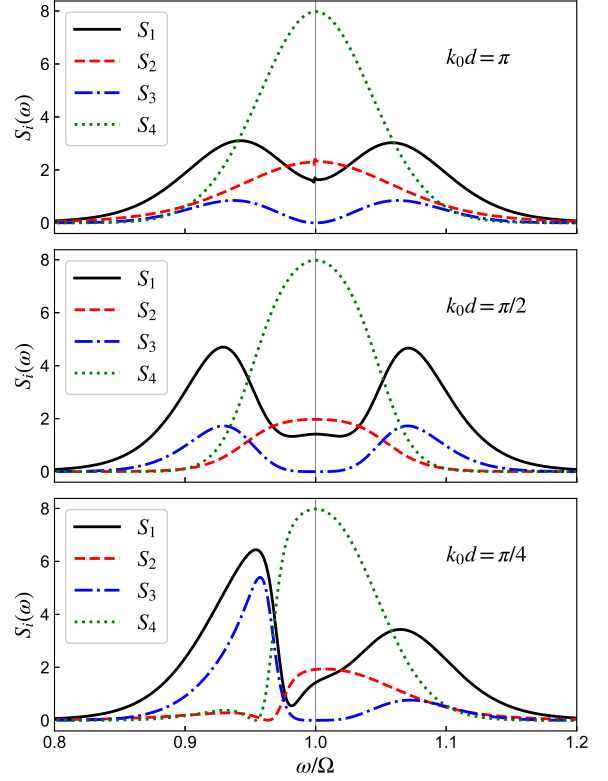


FIG. 11: Photon radiation spectra of a two-qubit system in 1D waveguide for incident Gaussian pulse. All plots show both transmitted ($S_1 = |\gamma_{WW}(\omega, t \rightarrow \infty)|^2\Omega$, $S_3 = |\gamma(\omega, t \rightarrow \infty)|^2\Omega$) and reflected ($S_2 = |\delta_{WW}(\omega, t \rightarrow \infty)|^2\Omega$, $S_4 = |\delta(\omega, t \rightarrow \infty)|^2\Omega$) radiation for three inter-qubit distances $\lambda/2$, $\lambda/4$ and $\lambda/8$. Solid (black) and dashed (red) lines represent the exact solutions (63) and (64), dotted-dashed (blue) and dotted (green) lines represent the approximate solutions (61), (62). The parameters of the qubit system and initial pulse are: $\omega_S/\Omega = 1$, $\Gamma/\Omega = 0.1$, $\Delta/\Omega = 0.1$.

side-peaks. However, as the coupling strength increases, all peaks became wider, and for $\Gamma/\Omega = 0.1$ central peak is barely recognizable. Although, its amplitude does not change and Γ only affects it's width, unlike the side-peaks which become both wider and smaller.

In Fig. 13 we show how photon spectra is changed for different width Δ of incident Gaussian pulse. When the initial pulse is very narrow, $\Delta/\Omega = 0.02$, the side-peaks of familiar transmission spectrum are almost zero, while the central peak is presented distinctly. By increasing pulse width, the side-peaks begin to grow, and the central peak, on the contrary, is getting smaller. This property of spectral line is different from Fig. 12: by increasing coupling strength Γ , central peak remains relatively the same, and change affects only side-peaks; by increasing width of incident pulse Δ , the central peak becomes smaller, and the side-peaks becomes larger.

Finally, in Fig. 14 we show, how spectra are changed if one shift the central frequency ω_S of incident pulse. As expected, this leads to symmetry shift to the right for

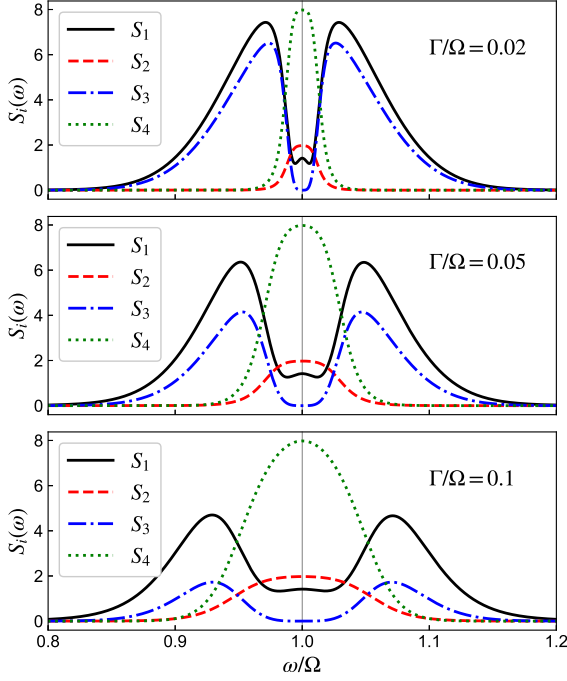


FIG. 12: Photon radiation spectra of a two-qubits for different coupling rates Γ/Ω . All plots show both transmitted ($S_1 = |\gamma_{WW}(\omega, t \rightarrow \infty)|^2\Omega$, $S_3 = |\gamma(\omega, t \rightarrow \infty)|^2\Omega$) and reflected ($S_2 = |\delta_{WW}(\omega, t \rightarrow \infty)|^2\Omega$, $S_4 = |\delta(\omega, t \rightarrow \infty)|^2\Omega$) radiation spectra. Solid (black) and dashed (red) lines represent the exact solutions (63) and (64), dotted-dashed (blue) and dotted (green) lines represent the approximate solutions (61), (62). The parameters of the qubit system and initial pulse are: $\omega_S/\Omega = 1$, $\Delta/\Omega = 0.1$, $k_0d = \pi/2$.

$\omega_S/\Omega = 1.05$ and to the left for $\omega_S/\Omega = 0.95$. However, one still can recognize the three-peak shape of spectral line for transmission spectra S_1 .

From the above figures we may have impression that the radiation spectra are rather smooth and regular as the function of frequency. However, the picture is much more complicated. For some "irregular" values of k_0d the radiation spectra show very different behavior. This kind of spectra are shown in Fig.15 for $k_0d = 0.125\pi$ ($d = \lambda/16$), $k_0d = 1.125\pi$ ($d = 9\lambda/16$), $k_0d = 2.125\pi$ ($d = 17\lambda/16$), $k_0d = 3.125\pi$ ($d = 25\lambda/16$). First, we notice in the top panel of Fig.15 that the transmission S_1 has a deep dip near the resonant frequency. This dip differs from zero by several thousandths. Other panels in Fig.15 also show the more shallow dips for S_1 . Second, to the left of the dips in three panels in Fig.15 we observe very sharp and narrow peaks for transmission radiation S_1 . The peak at the bottom panel in Fig.15 ($k_0d = 3.125\pi$) has its maximum at 14.7 which is not shown in the panel. These narrow peaks are clear signature of the effects of non-Markovianity and subradiant transitions, which yields the ultra narrow emission lines.

For every plot in Fig.11-Fig.15 we controlled the normalizing quantity $I = \int d\omega |\gamma_{WW}(\omega)|^2 + \int d\omega |\delta_{WW}(\omega)|^2$

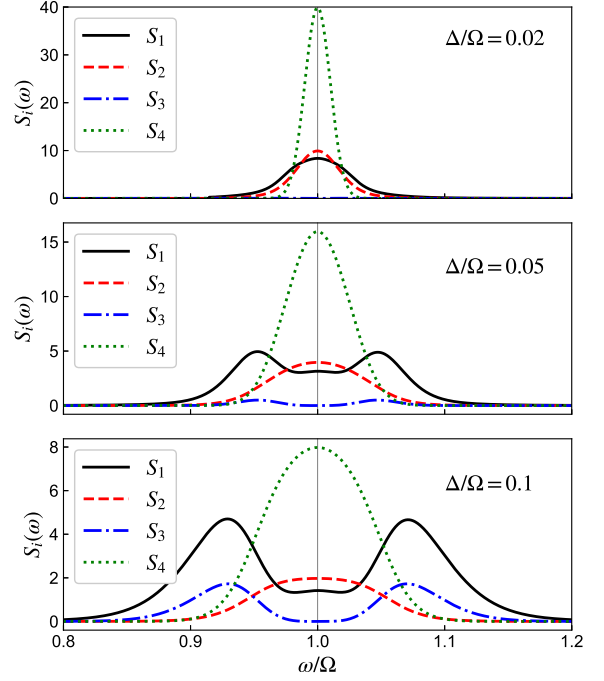


FIG. 13: Photon radiation spectra of a two-qubit system for different widths Δ/Ω of incident Gaussian pulse. All plots show both transmitted ($S_1 = |\gamma_{WW}(\omega, t \rightarrow \infty)|^2\Omega$, $S_3 = |\gamma(\omega, t \rightarrow \infty)|^2\Omega$) and reflected ($S_2 = |\delta_{WW}(\omega, t \rightarrow \infty)|^2\Omega$, $S_4 = |\delta(\omega, t \rightarrow \infty)|^2\Omega$) radiation spectra. Solid (black) and dashed (red) lines represent the exact solutions (63) and (64), dotted-dashed (blue) and dotted (green) lines represent the approximate solutions (61), (62). The parameters of the qubit system and initial pulse are $\omega_S/\Omega = 1$, $\Gamma/\Omega = 0.1$, $k_0d = \pi/2$.

where the integration was performed within the frequency span of the plots. In every case, I differed from unity less than several thousandths.

VI. SUMMARY

In this paper we analyze the scattering of a single-photon pulse by a one-dimensional chain of two level artificial atoms (qubits) embedded in an open waveguide. The system is described by the continuum mode Jaynes-Cummings Hamiltonian with Hilbert space being truncated to a single excitation subspace. By solving the nonstationary Schrodinger equation we derive a time-dependent dynamical equations for qubits' amplitudes and for transmitted and reflected photon spectra. Unlike previous approaches our calculations are performed only for physical, positive, frequency axis. This significantly changes the dynamics of the system. First, it leads to the additional photon-mediated dipole-dipole interaction between qubits which results in the violation of the phase coherence between them. Second, the spectral lines of transmitted and reflected spectra crucially depend on the shape of incident pulse. We apply our theory to one-qubit

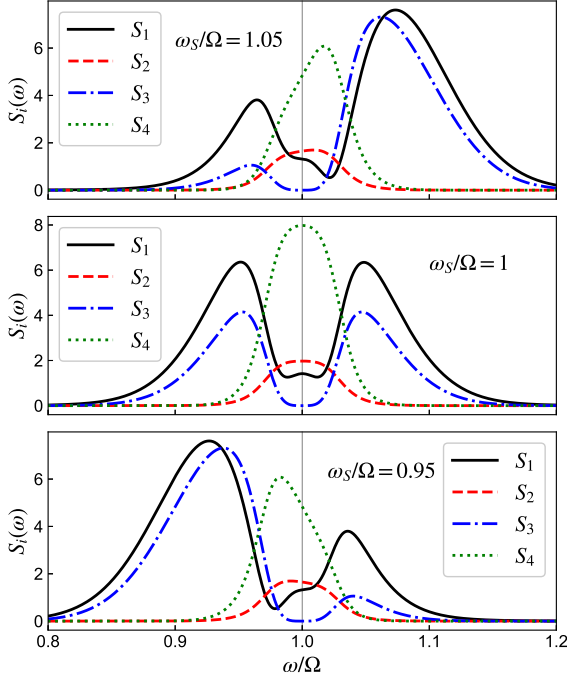


FIG. 14: Photon radiation spectra of a two-qubit system when central frequency ω_S/Ω of incident Gaussian pulse is not equal to resonant frequency of the qubits. All plots show both transmitted ($S_1 = |\gamma_{WW}(\omega, t \rightarrow \infty)|^2\Omega$, $S_3 = |\gamma(\omega, t \rightarrow \infty)|^2\Omega$) and reflected ($S_2 = |\delta_{WW}(\omega, t \rightarrow \infty)|^2\Omega$, $S_4 = |\delta(\omega, t \rightarrow \infty)|^2\Omega$) radiation spectra. Solid (black) and dashed (red) lines represent the exact solutions (63) and (64), dotted-dashed (blue) and dotted (green) lines represent the approximate solutions (61), (62). The parameters of the qubit system and initial pulse are: $\Gamma/\Omega = 0.05$, $\Delta/\Omega = 0.1$, $k_0d = \pi/2$.

and two-qubit systems. For these two cases we obtain the explicit expressions for the qubits' amplitudes and for the photon spectra. For the travelling incident Gaussian wave packet we calculate the line shapes of transmitted and reflected photons. We show that the transmitted and reflected photon spectra crucially depend on the initial distance of the Gaussian peak from the first qubit. As this distance becomes closer to the qubit, the spectral lines more and more deviate from known results where the continuation of the qubit-photon interaction to the negative frequency axis is used.

We believe that the results obtained in the paper may be important for the practical implementation in waveguide QED problems with superconducting qubits where the control and readout pulse generators should be placed as close as possible to the qubit chip at millikelvin temperatures [39].

Our approach can also be further extended and applied to the single-photon scattering by multi-level qubits in strong light-matter coupling regimes.

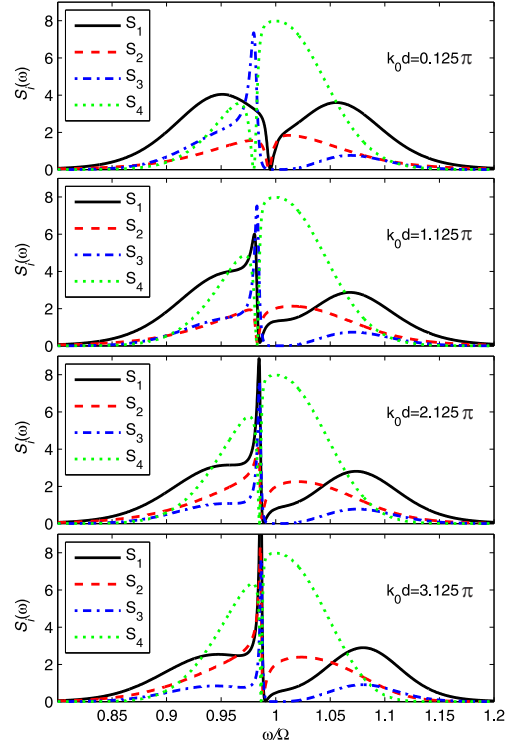


FIG. 15: Photon radiation spectra of a two-qubit system for different values of k_0d . All plots show both transmitted ($S_1 = |\gamma_{WW}(\omega, t \rightarrow \infty)|^2\Omega$, $S_3 = |\gamma(\omega, t \rightarrow \infty)|^2\Omega$) and reflected ($S_2 = |\delta_{WW}(\omega, t \rightarrow \infty)|^2\Omega$, $S_4 = |\delta(\omega, t \rightarrow \infty)|^2\Omega$) radiation spectra. Solid (black) and dashed (red) lines represent the exact solutions (63) and (64), dotted-dashed (blue) and dotted (green) lines represent the approximate solutions (61), (62). The parameters of the qubit system and initial pulse are: $\Gamma/\Omega = 0.1$, $\Delta/\Omega = 0.1$, $\omega_S = \Omega$.

Acknowledgments

The authors thank O. V. Kibis and A. N. Sultanov for fruitful discussions. The work is supported by the Ministry of Science and Higher Education of Russian Federation under the project FSUN-2023-0006. O. Chuikin acknowledges the financial support from the Foundation for the Advancement of Theoretical Physics and Mathematics “BASIS”.

Appendix A: Derivation of equation (28)

We begin with the integral in equation (26):

$$I(\nu) = \int_0^\infty d\omega g^2(\omega) \cos(k(x_n - x_{n'})) \zeta(\nu - \omega). \quad (\text{A1})$$

Using (25) we obtain:

$$\begin{aligned} I(\nu) &= -i\pi g^2(\nu) \cos k_\nu d_{nn'} + I_-(\nu) \\ &= -i\pi g^2(\nu) e^{ik_\nu d_{nn'}} + (I_-(\nu) - \pi g^2(\nu) \sin k_\nu d_{nn'}), \end{aligned} \quad (\text{A2})$$

where:

$$I_-(\nu) = -P \int_0^\infty d\omega \frac{g^2(\omega) \cos(kd_{nn'})}{\omega - \nu}. \quad (\text{A3})$$

Usually, this integral is calculated by taking $g^2(\omega)$ out of the integral at the frequency ν and moving the lower bound to $-\infty$:

$$I_-(\nu) \approx -g^2(\nu) P \int_{-\infty}^\infty d\omega \frac{\cos(\omega t_{nn'})}{\omega - \nu} = \pi g^2(\nu) \sin(\nu t_{nn'}), \quad (\text{A4})$$

where $t_{nn'} = d_{nn'}/v_g$ and we used Kramers-Kronig relation. In this case the second term in brackets in (A2) is zero. Therefore, for $I(\nu)$ we obtain: $I(\nu) = -i\pi g^2(\nu) \exp(i\nu t_{nn'})$.

We would obtain (A4) if we added to $I_-(\nu)$ (A3) the non-RWA counter rotating term $I_+(\nu)$:

$$I_+(\nu) = -P \int_0^\infty d\omega \frac{g^2(\omega) \cos(kd_{nn'})}{\omega + \nu}. \quad (\text{A5})$$

If we assume $g^2(\omega) = \lambda\omega$, change variables in the integrand in (A5) ($\omega \rightarrow -\omega$), and add the result to $I_-(\nu)$ we obtain the result which is given in (A4). Strictly speaking, this procedure is not well justified because any frequency dependent coupling ($g^2(\omega)$ in our case) must be exactly zero for negative frequencies.

In order to estimate the contribution from non RWA term more elaborate calculation of $I_-(\nu)$ (A3) is necessary. First, we add and subtract to $I_-(\nu)$ the counter rotating term $I_+(\nu)$: $I_-(\nu) = [I_-(\nu) + I_+(\nu)] - I_+(\nu) = \pi g^2(\nu) \sin(\nu t_{nn'}) - I_+(\nu)$. Therefore, for the second term in right hand side in (A2) we obtain:

$$I_+(\nu) = - (I_-(\nu) - \pi g^2(\nu) \sin k_\nu d_{nn'}). \quad (\text{A6})$$

Next, we begin calculating the quantity $I_+(\nu)$. We assume $g^2(\omega) = \lambda\omega$. Then, for $I_+(\nu)$ we obtain:

$$\begin{aligned} I_+(\nu) &= -\lambda P \int_0^\infty d\omega \frac{\omega \cos(\omega t_{nn'})}{\omega + \nu} \\ &= -\lambda \int_0^\infty d\omega \cos(\omega t_{nn'}) + \lambda \nu P \int_0^\infty d\omega \frac{\cos(\omega t_{nn'})}{\omega + \nu}. \end{aligned} \quad (\text{A7})$$

To calculate the first term of the right-hand side, we add a small converging factor. This reflects the fact that

the system does not respond at high frequencies. In this way, we find that this term vanishes:

$$\begin{aligned} \int_0^\infty d\omega \cos(\omega t_{nn'}) &= \nu \int_0^\infty dy \cos(y \nu t_{nn'}) \\ &= \nu \lim_{\eta \rightarrow 0^+} \int_0^\infty dy e^{-\eta y} \cos y \nu t_{nn'} = \nu \lim_{\eta \rightarrow 0^+} \frac{\eta}{(\nu t_{nn'})^2 + \eta^2} = 0. \end{aligned} \quad (\text{A8})$$

In the integrand of the second term we change variable $x = (\omega + \nu)/\nu$:

$$\begin{aligned} P \int_0^\infty d\omega \frac{\cos(\omega t_{nn'})}{\omega + \nu} &= P \int_1^\infty dx \frac{\cos((x-1)\nu t_{nn'})}{x} \\ &= \cos \nu t_{nn'} P \int_1^\infty dx \frac{\cos(x \nu t_{nn'})}{x} \\ &\quad + \sin \nu t_{nn'} P \int_1^\infty dx \frac{\sin(x \nu t_{nn'})}{x}. \end{aligned} \quad (\text{A9})$$

Two integrals in (A9) can be expressed in terms of sine and cosine integral functions which are given in (29). Therefore, for the quantity $I_+(\nu)$ we obtain:

$$\begin{aligned} I_+(\nu) &= -g^2(\nu) \cos \nu t_{nn'} Ci(\nu |t_{nn'}|) \\ &\quad + g^2(\nu) \sin \nu t_{nn'} \left(\frac{\pi}{2} \text{sgn}(t_{nn'}) - Si(\nu t_{nn'}) \right). \end{aligned} \quad (\text{A10})$$

As is seen from (A10), the quantity $I_+(\nu)$ is the even function of $t_{nn'}$. Therefore we may rewrite (A10) in the following form:

$$\begin{aligned} I_+(\nu) &= -g^2(\nu) \cos \nu t_{nn'} Ci(\nu |t_{nn'}|) \\ &\quad + g^2(\nu) \sin \nu |t_{nn'}| \left(\frac{\pi}{2} - Si(\nu |t_{nn'}|) \right). \end{aligned} \quad (\text{A11})$$

Finally, for $I(\nu)$ we obtain:

$$\begin{aligned} I(\nu) &= -i \frac{\Gamma(\nu)}{4} e^{i\nu |t_{nn'}|} + \frac{\Gamma(\nu)}{4\pi} \cos \nu t_{nn'} Ci(\nu |t_{nn'}|) \\ &\quad + \frac{\Gamma(\nu)}{4\pi} \sin \nu |t_{nn'}| \left(-\frac{\pi}{2} + Si(\nu |t_{nn'}|) \right). \end{aligned} \quad (\text{A12})$$

The insertion of $I(\nu)$ in (26) provides the equation (27) with the quantity $G(kd_{nn'})$ defined in (28).

In fact, according to the derivation the quantity $G(kd_{nn'})$ can be expressed as:

$$G(k_\nu d_{nn'}) = -\frac{4}{\Gamma(\nu)} I_+(\nu) = -\frac{4}{\Gamma(\nu)} \int_0^\infty d\omega \frac{g^2(\omega) \cos k_\nu d_{nn'}}{\omega + \nu}. \quad (\text{A13})$$

Simply speaking, $G(kd_{nn'})$ is the difference between $\pi g^2(\nu) \sin(\nu t_{nn'})$ which accounts for the non RWA contribution ($\pi g^2(\nu) \sin(\nu t_{nn'}) = I_-(\nu) + I_+(\nu)$) and $I_-(\nu)$:

$$G(kd_{nn'}) = -\frac{4}{\Gamma(\nu)} (\pi g^2(\nu) \sin(\nu t_{nn'}) - I_-(\nu)). \quad (\text{A14})$$

The numerical calculations of $G(kd)$ which are presented in Figs. 7, 8, 9 in the main text show that within resonance width the non-RWA contribution is rather small for $kd_{nn'} > \pi/4$. However, this is not the case if $kd_{nn'} < \pi/4$.

Appendix B: Proof of equation (36)

In the Wigner-Weisskopf approximation $\Gamma(\Omega) \ll \Omega$. Therefore, in (35) we may ignore $F(\omega)$ and replace $\Gamma(\omega)$ with $\Gamma(\Omega) \equiv \Gamma$. Further, we use for $\zeta(\omega - \omega')$ one of its representation:

$$\zeta(\omega - \omega') = \lim_{\sigma \rightarrow 0} \frac{1}{\omega - \omega' + i\sigma}. \quad (\text{B1})$$

Therefore, for (35) we obtain:

$$\begin{aligned} \beta(t) &= i \int_0^\infty d\omega' g(\omega') \gamma_0(\omega') \\ &\times \lim_{\sigma \rightarrow 0} \int_{-\infty}^\infty \frac{d\omega}{2\pi} \frac{e^{-i(\omega - \Omega)t}}{(\omega - \Omega + i\frac{\Gamma}{2})(\omega - \omega' + i\sigma)}. \end{aligned} \quad (\text{B2})$$

There are only two poles in the lower part of the complex ω plane. Applying the Cauchy residue theorem to the second integral in (B2) we obtain the following result:

$$\beta(t) = \int_0^\infty d\omega' g(\omega') \gamma_0(\omega') \frac{e^{-\frac{\Gamma}{2}t} - e^{-i(\omega' - \Omega)t}}{(\omega' - \Omega + i\frac{\Gamma}{2})}, \quad (\text{B3})$$

for $t > 0$ and $\beta(t) = 0$ for $t < 0$.

-
- [1] J. M. Raimond, M. Brune, and S. Haroche, Manipulating quantum entanglement with atoms and photons in a cavity, *Rev. Mod. Phys.* **73**, 565 (2001)., 565 (2001).
 - [2] D. Roy, C. M. Wilson, and O. Firstenberg, Strongly interacting photons in one-dimensional continuum *Rev. Mod. Phys.* **89**, 021001 (2017).
 - [3] X. Gu, A. F. Kockum, A. Miranowicz, Y.-X. Liu, and F. Nori, Microwave photonics with superconducting quantum circuits, *Phys. Rep.* **718**, 1 (2017).
 - [4] A. S. Sheremet, M. I. Petrov, I. V. Iorsh, A. V. Poshakinskiy, and A. N. Poddubny, Waveguide quantum electrodynamics: Collective radiance and photon-photon correlations. *Rev. Mod. Phys.* **95**, 015002 (2023).
 - [5] D. Leibfried, R. Blatt, C. Monroe, and D. Wineland, Quantum dynamics of single trapped ions. *Rev. Mod. Phys.* **75**, 281 (2003).
 - [6] X. L. Wang, Y. H. Luo, H. L. Huang, M.-C. Chen, Zu-En Su, C. Liu, C. Chen, W. Li, Yu-Q. Fang, X. Jiang, J. Zhang, L. Li, N.-L. Liu, C.-Y. Lu, and J.-W. Pan, 18-qubit entanglement with six photons three degrees of freedom. *Phys. Rev. Lett.* **120**, 260502 (2018).
 - [7] X. L. Wang, L. K. Chen, W. Li, H.-L. Huang, C. Liu, C. Chen, Y.-H. Luo, Z.-E. Su, D. Wu, Z.-D. Li, H. Lu, Y. Hu, X. Jiang, C.-Z. Peng, L. Li, N.-L. Liu, Yu-Ao Chen, Chao-Yang Lu, and Jian-Wei Pan, Experimental ten-photon entanglement. *Phys. Rev. Lett.* **117**, 210502 (2016).
 - [8] V. Verma, D. Yadav, D. K. Mishra Improvement on cyclic controlled teleportation by using a seven-qubit entangled state. *Optical and Quantum Electronics* **53**, 448 (2021).
 - [9] N. Samkharadze, G. Zheng, N. Kalhor, D. Brousse, A. Sammak, U. C. Mendes, A. Blais, G. Scappucci, and L. M. K. Vandersypen, Strong spin-photon coupling in silicon, *Science* **359**, 1123 (2018).
 - [10] R. Khordad and H. R. Rastegar Sedehi, Comparison of bound magneto-polaron in circular, elliptical, and triangular quantum dot qubit. *Optical and Quantum Electronics* **52**, 428 (2020).
 - [11] P. Krantz, M. Kjaergaard, F. Yan, T. P. Orlando, S. Gustavsson, and W. D. Oliver, A quantum engineer's guide to superconducting qubits. *Appl. Phys. Rev.* **6**, 021318 (2019).
 - [12] M. Kjaergaard, M. E. Schwartz, J. Braumüller, P. Krantz, Joel I.-J. Wang, S. Gustavsson, and W. D. Oliver, Superconducting qubits: current state of play. *Ann. Rev. Condensed Matter Phys.* **11**, 369 (2019).
 - [13] J. Ruostekoski and J. Javanainen, Arrays of strongly coupled atoms in a one-dimensional waveguide. *Phys. Rev. A* **96**, 033857 (2017).
 - [14] K. Lalumière, B. C. Sanders, A. F. van Loo, A. Fedorov, A. Wallraff, and A. Blais, Input-output theory for waveguide QED with an ensemble of inhomogeneous atoms. *Phys. Rev. A* **88**, 043806 (2013).
 - [15] D. E. Chang, L. Jiang, A. V. Gorshkov, and H. J. Kimble, Cavity QED with atomic mirrors. *New J. Phys.* **14**, 063003 (2012).
 - [16] M. Mirhosseini, E. Kim, X. Zhang, A. Sipahigil, P. B. Dieterle, A. J. Keller, A. Asenjo-Garcia, D. E. Chang, and O. Painter, Cavity quantum electrodynamics with atom-like mirrors. *Nature* **569**, 692 (2019).
 - [17] J. D. Brehm, A. N. Poddubny, A. Stehli, T. Wolz, H. Rotzinger, and A. V. Ustinov, Waveguide bandgap engineering with an array of superconducting qubits, *npj Quantum Materials* **6**, 10 (2021).
 - [18] A. F. van Loo, A. Fedorov, K. Lalumière, B. C. Sanders, A. Blais, and A. Wallraff Photon-mediated interactions between distant artificial atoms. *Science* **342**, 1494 (2014).
 - [19] J.-T. Shen and S. Fan, Theory of single-photon transport in a single-mode waveguide. I. Coupling to a cavity

- containing a two-level atom. *Phys. Rev. A* **79**, 023837 (2009).
- [20] M.-T. Cheng, J. Xu, and G. S. Agarwal, Waveguide transport mediated by strong coupling with atoms. *Phys. Rev. A* **95**, 053807 (2017).
- [21] Y.-L. L. Fang, H. Zheng, and H. U. Baranger, One-dimensional waveguide coupled to multiple qubits photon-photon correlations. *EPJ Quantum Technol.* **1**, 3 (2014).
- [22] H. Zheng and H. U. Baranger, Persistent Quantum Beats and Long-Distance Entanglement from Waveguide-Mediated Interactions. *Phys. Rev. Lett.* **110**, 113601 (2013).
- [23] D. Roy, Correlated few-photon transport in one-dimensional waveguides: Linear and nonlinear dispersions, *Phys. Rev. A* **83**, 043823 (2011).
- [24] J.-F. Huang, T. Shi, C. P. Sun, and F. Nori, Controlling single-photon transport in waveguides with finite cross section, *Phys. Rev. A* **88**, 013836 (2013).
- [25] G. Diaz-Camacho, D. Porras, and J. J. Garcia-Ripoll, Photon-mediated qubit interactions in one-dimensional discrete and continuous models. *Phys. Rev. A* **91**, 063828 (2015).
- [26] S. Fan, S. E. Kocabas, and J.-T. Shen, Input-output formalism for few-photon transport in one-dimensional nanophotonic waveguides coupled to a qubit, *Phys. Rev. A* **82**, 063821 (2010).
- [27] A. H. Kiielerich and K. Molmer, Input-Output Theory with Quantum Pulses. *Phys. Rev. Lett.* **123**, 123604 (2019).
- [28] Ya. S. Greenberg and A. A. Shtygashev, Non hermitian Hamiltonian approach to the microwave transmission through a one-dimensional qubit chain. *Phys. Rev. A* **92**, 063835 (2015).
- [29] Ya. S. Greenberg, A. A. Shtygashev, and A. G. Moiseev, Waveguide band-gap N-qubit array with a tunable transparency resonance. *Phys. Rev. A* **103**, 023508 (2021).
- [30] T. S. Tsoi and C. K. Law, Quantum interference effects of a single photon interacting with an atomic chain. *Phys. Rev. A* **78**, 063832 (2008).
- [31] Y. Chen, M. Wubs, J. Mork, and A. F. Koendrink, Coherent single-photon absorption by single emitters coupled to one-dimensional nanophotonic waveguides, *New J. Phys.* **13**, 103010 (2011).
- [32] Z. Liao, X. Zeng, S.-Y. Zhu, and M. S. Zubairy, Single-photon transport through an atomic chain coupled to a one-dimensional nanophotonic waveguide. *Phys. Rev. A* **92**, 023806 (2015).
- [33] Z. Liao, H. Nha, and M. S. Zubairy, Dynamical theory of single-photon transport in a one-dimensional waveguide coupled to identical and nonidentical emitters. *Phys. Rev. A* **94**, 053842 (2016).
- [34] Z. Liao, X. Zeng, H. Nha, and M. S. Zubairy, Photon transport in a one-dimensional nanophotonic waveguide QED system *Phys. Scr.* **91**, 063004 (2016).
- [35] C. Zhou, Z. Liao, and M. S. Zubairy, Decay of a single photon in a cavity with atomic mirrors. *Phys. Rev. A* **105**, 033705 (2022).
- [36] A. Gonzalez-Tudela and D. Porras, Mesoscopic Entanglement Induced by Spontaneous Emission in Solid-State Quantum Optics, *Phys. Rev. Lett.* **110**, 080502 (2013).
- [37] C. Cohen-Tannoudji, J. Dupont-Roc, and G. Grynberg, Atom-photon interactions. Basic processes and applications. Wiley-VCH GmbH and Co. 2004, p.244.
- [38] Ya. S. Greenberg, A. A. Shtygashev, and A. G. Moiseev, Spontaneous decay of artificial atoms in a three-qubit system. *Eur. Phys. J.* **B94**, 221 (2021).
- [39] F. Lecocq, F. Quinlan, K. Cicak, J. Aumentado, S. A. Diddams, J. D. Teufel, Control and readout of a superconducting qubit using a photonic link. *Nature* **591**, 575 (2021).
- [40] K. J. Blow, R. Loudon, and S. J. D. Phoenix, Continuum fields in quantum optics. *Phys. Rev. A* **42**, 4102 (1990).
- [41] P. Domokos, P. Horak, and H. Ritsch, Quantum description of light-pulse scattering on a single atom in waveguides. *Phys. Rev. A* **65**, 033832 (2002).
- [42] W. Heitler, *The Quantum Theory of Radiation* (Oxford University Press, Oxford, 1954).
- [43] I.M. Sokolov, D. V. Kupriyanov, and M.D. Havey, Microscopic Theory of Scattering of Weak Electromagnetic Radiation by a Dense Ensemble of Ultracold Atoms. *J. Exp. Theor. Phys.* **112**, 246 (2011).
- [44] A. S. Kuraptsev and I. M. Sokolov, Reflection of resonant light from a plane surface of an ensemble of motionless point scatterers: Quantum microscopic approach. *PRA* **91**, 053822 (2015).
- [45] A. S. Kuraptsev and I. M. Sokolov Microscopic Theory of Dipole-Dipole Interaction in Ensembles of Impurity Atoms in a Fabry-Perot Cavity. *J. Exp. Theor. Phys.* **123**, 237 (2016).
- [46] Ya. S. Greenberg, A. G. Moiseev, and A. A. Shtygashev, Single-photon scattering on a qubit: Space-time structure of the scattered field. *Phys. Rev. A* **107**, 013519 (2023).
- [47] S. Derouault and M. A. Bouchene, One-photon wave packet interacting with two separated atoms in a one-dimensional waveguide: Influence of virtual photons. *Phys. Rev. A* **90**, 023828 (2014).
- [48] J.-T. Shen and S. Fan, Coherent photon transport from spontaneous emission in one-dimensional waveguides, *Optics Letters* **30**, 2001 (2005).
- [49] J. T. Shen and S. Fan, Coherent Single Photon Transport in a One-Dimensional Waveguide Coupled with superconducting Quantum Bits, *Phys. Rev. Lett.* **95**, 213001 (2005).
- [50] S. Derouault and M. A. Bouchene, One-photon wave packet interacting with two separated atoms in a one-dimensional waveguide: Influence of virtual photons. *Phys. Rev. A* **90**, 023828 (2014).